

## REPAIR CONNECTION WITH WOODEN WEDGED DOWELS: AXIAL TENSILE AND SHEAR VERIFICATIONS.

Elena Perria<sup>1</sup>, Mike Sieder<sup>2</sup>, Svenja Siegert<sup>3</sup>, Cordula Reulecke<sup>4</sup>

**ABSTRACT:** The present paper describes the final results of the research project by the title “Repair connection with wooden wedged dowels. New and alternative repair method that meets the demands of Monument Protection of built substance’s gentle care and material fairness”. The project aims to develop guidelines for static-constructive use of wood-wood (carpentry) repair connections with wooden wedged dowels as mechanical fasteners. In this paper the boundary conditions and the axial tensile and shear verifications are presented.

**KEYWORDS:** carpentry connections, mechanical fasteners, wooden wedged dowels, axial tensile verification, shear verification

### 1 INTRODUCTION

In case of repair or replacement of damaged cross sections in historical timber buildings, metal fasteners like screws and bolts are very often used, especially if the fasteners have to be designed for planned shear or tensile stress, or a clamping effect in the wood-wood connection is required. Another common solution is bonding of steel or plastic rods that realize the connection with the existing structural members by means of synthetic resin grouting, glue, etc. e.g. the so-called Beta-system [1], among others. However, these repair methods and techniques are not to be favored from the point of view of monument preservation [2, 3]. Material conformity and appropriate, durable, repair methods according to the ICOMOS principles [2, 3] play a crescent role as a requirement in the future. In the Charter of Mexico [4] is stated that (a) *traditional wood-wood connections as repair connections are prioritized, while globally recognized as effective, and part of global competences in heritage conservation.* (b) *Non-material conforming techniques have not proven themselves in practice, and their long-term effects on historic wood structures are not sufficiently known; therefore, they are not to be favored.* This latter statement (b) was mitigated in the 1999’s *Principles for the conservation of wooden built heritage* [5], presented as revision of the Charter of Mexico [4]. Nevertheless, long-term damages can occur when non-conform repair techniques are used [1, 6–8]. The most common damages are chemical effects (e.g. corrosion) on metal fasteners that transfer the oxidation on wood [6], and water condensation in the contact area between plastic or steel fasteners with the cross section, that promotes rot in wood [8]. Comprehensive challenges in the preservation of monuments are increasingly appearing because of improperly carried out renovations in the past decades.

This represents a considerable economic factor that greatly increases the expenses for the care and preservation of our architectural heritage [6]. For all these reasons, since two decades, the monument preservation office in southern Lower Saxony, Germany have been made many attempts to reduce the use of metal fasteners/ bonding rods in the repair of wooden structures, and to foster wood-wood connections as repair connections. On the other side, structural engineers are oft unable - due to the lack of calculation basis - to provide a verification for many traditional wood-wood connections; therefore, they are oft not realized.

The aim the research presented in this paper is the development of some necessary engineering tools to perform the verification of carpentry repair connections with wooden wedged dowels as mechanical fasteners (Figure 4) under axial tensile and shear load.

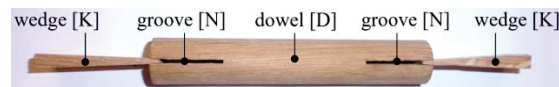


**Figure 1:** Components of a wooden wedged dowel (WWD)

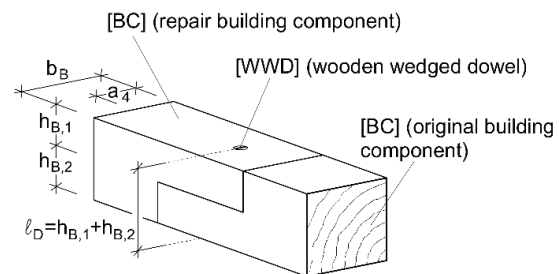


**Figure 2:** Illustration of the repair connection with wooden wedged dowel (example of use in a single-shear connection)

<sup>1</sup> Elena Perria, iBHolz Technische Universität Braunschweig, Germany, e.perria@tu-braunschweig.de

<sup>2</sup> Mike Sieder, iBHolz Technische Universität Braunschweig, Germany, m.sieder@tu-braunschweig.de

<sup>3</sup> Svenja Siegert, IGP Gockel PartGmbH - Ingenieure und Architektin, Germany, siegert.svenja@gockel-ingenieure.de

<sup>4</sup> Cordula Reulecke, Niedersächsisches Landesamt für Denkmalpflege, Regionalreferat Braunschweig, Germany, Cordula.Reulecke@nld.niedersachsen.de

## 2 METHODOLOGY

In the performed research project [9], the hypothesis about the use of the wooden wedged dowels in the load cases shear and axial tensile load was pursued experimentally, numerically and analytically. With reference to existing theories and verification methods on wooden fasteners [10–14], systematic first-approach tests TV1 [15] were developed. The aim was to define geometric-constructive parameters like crack formation, edge distances and penetration depth. In a second step, the investigated geometric-constructive parameters were classified according to their influence on the mechanical behaviour and on load-carrying capacity, in order to define the geometric-constructive framework for a static verification of the repair connection under axial tensile and shear loading. The firstly assumed hypotheses about the geometric-constructive parameters of the wooden wedged dowels [15] were adapted to the new findings and boundary conditions were defined (tests TV2 in [9]). The results generated so far were confirmed numerically, basing on the finite element method, and experimentally. Carpentry connections with wooden wedged dowels were tested under axial tensile (tests V1 [9]) and double shear loading (tests SV1 [9]), and the characteristic values of the load-bearing capacity were further used for the development of following verifications.

## 3 GEOMETRY

In order to obtain the expected results in terms of characteristic values of strength and remain in the average of the tested failure modes, general manufacturing rules and geometry features are defined. In the following Table 1, Figure 3 are explained the geometric/constructive parameters and boundary conditions in the repair connection. More information about these parameters is contained in [15].

**Table 1:** Parameters of the wooden wedged dowel

Symbol	Description of the parameter
H	Wood species combination: Dowel / Building Component (BC)
H1	Dowel: <i>Quercus</i> / BC: <i>Picea abies</i>
H2	Dowel: <i>Quercus</i> / BC: <i>Quercus</i>
H3	Dowel: <i>Fraxinus excelsior</i> / BC: <i>Picea abies</i>
T1	Angle $\theta$ between groove's orientation and direction of the annual rings on dowel's cross section T1-0 $\rightarrow \theta = 0^\circ$
T2	Angle $\varphi$ between groove's orientation on Side 1 [N,1] and fibers' direction on building component's surface T2-90 $\rightarrow \varphi = 90^\circ$
G	Angle $\beta$ between groove's orientation on Side 1 [N,1] and on Side 2 [N,2] Orientation of the groove on S1 parallel to orientation on S2 [G//]

As explained in Figure 2 and Table 1 the repair connection is composed by the original and repair building components and one or more mechanical fasteners, the wooden wedged dowels. The tested combinations are reported in the Table 1. More general rules are (a) the wood species for the wedge is always oak (*Quercus*) or the wedge must have a minimum strength of D30 [16] (b) the dowel must have a higher bulk density than the one of both original and repair building components  $\rho_D \geq \rho_{BC}$ .

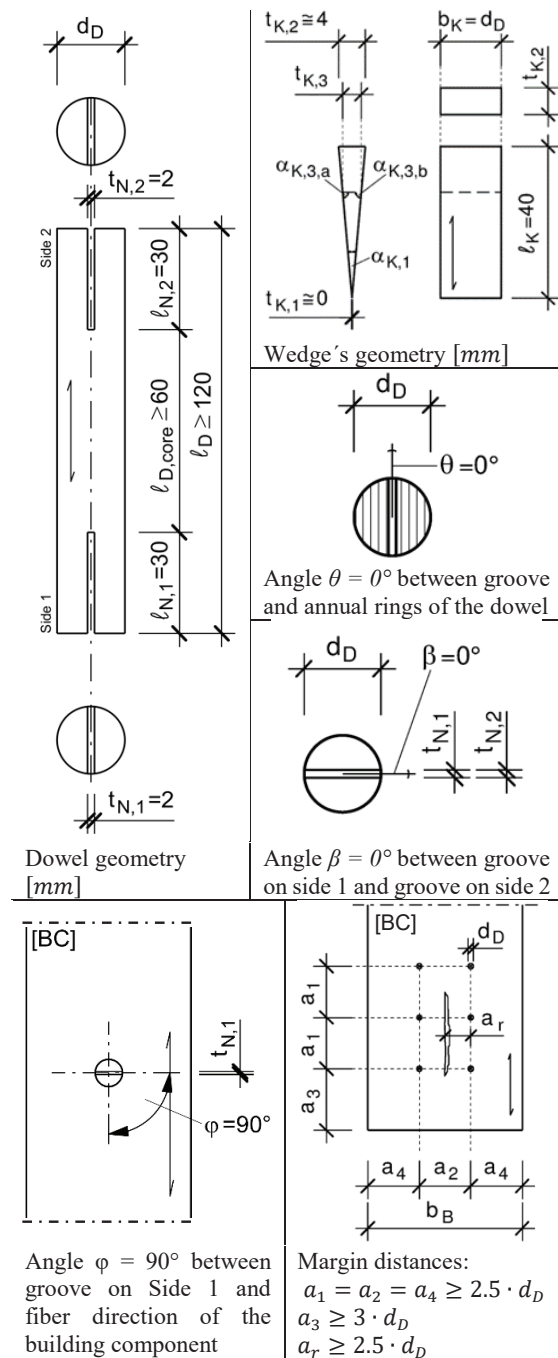


**Figure 3:** Geometric boundary conditions for the connection with wooden wedged dowels

### 3.1 BOUNDARY CONDITIONS AND WORKING PRINCIPLES OF THE FASTENER

The prerequisite for the transmission of load between fastener and cross section is a contact surface. A distinction is made between two types of contact surfaces for load transfer (Figure 4): A) Load-transfer effect due to wedging (spreading effect) area; B) Load-transfer effect due to skin friction area.

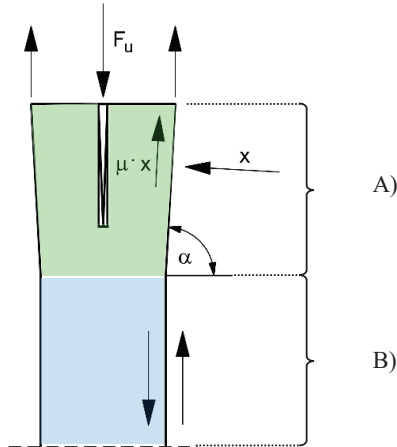


**Figure 4:** Mechanical model of the wooden wedged dowel under tensile stress. A) In green, load transfer area activated due to the wedging. B) In light blue, area of action of the skin friction.

The presented models consider a connection with wooden wedged dowel with idealized load-transfer areas. The load transfer in (A) is independent from manufacturing of connection, but dependent on the type of wood (or better, the wood combination) and the spreading angle  $\alpha$ . The load transfer in (B) depends on the manufacturing process and can only be guaranteed if the manufacturing is carried out without deviations from the required geometry (imperfections). As this latter cannot be guaranteed in case of hand-made connections, the skin friction area (B) is neglected in the proposed verification and is considered that the load-carrying capacity of the wooden wedged dowel is determined by the two wedged extremities with the load transfer type (A) (see Figure 4).

## 4 Results

### 4.1 VERIFICATION FOR THE REPAIR CONNECTION WITH WOOD WEDGED DOWELS UNDER AXIAL TENSILE LOAD

Starting point for the development of a mechanical model for repair connections with WWD under axial tensile load was the verification model for pile foundations. The relationship between pile displacement  $y$  and the horizontal stress  $\sigma_h$  applies here to  $\sigma_h = k_s \cdot y$  [17]. From experimental results V1 [9] is defined that the maximum displacement of the system is at the top of the wedging, on BC's surface, and it is defined as  $v(z=0) \neq 0$ . The displacement is reducing to zero along  $z$ -axis, in the direction of the center of the wedge. According to numerical simulations the displacement of the system is zero at a depth  $t_w$ , defined as  $v(z \geq t_w) = 0$ . This value

defines the depth of load transfer area (A) as in Figure 4. The distribution of the displacement causes a stress distribution that is maximum on BC's surface. Here, the real and idealized stress distribution is assumed as by Spörk in [18, 19] (see Figure 6, above). The maximum stress value on BC's surface is defined as  $\sigma_N(z=0) \neq 0$  (see Figure 6, below). The stress has a linear course and is reducing along the  $z$ -axis until the maximum depth of the wedging effect  $t_w$ . At a depth  $z \geq t_w$  the stress is zero  $\sigma_N(z \geq t_w) = 0$  and there is no more load transfer between the fastener and the BC's cross section (see Figure 5). Considering  $(x, y, z) \leftrightarrow (u, v, w)$ , the stress value  $\sigma_N(z)$  in the dowel is the one defined in the eq. (1).

$$\sigma_N(z) = k_s \cdot v(z) \quad \left[ \frac{\text{N}}{\text{mm}^2} \right] \quad (1)$$

with:

$\sigma_N(z)$  = stress value in the system along  $z$ -axis  
 $k_s$  = foundation modulus

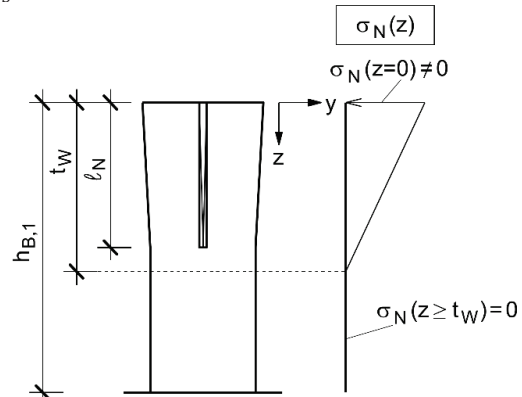


**Figure 5:** Mechanical model of the wooden wedged dowel. Distribution of stress along the  $z$ -axis due to wedging.

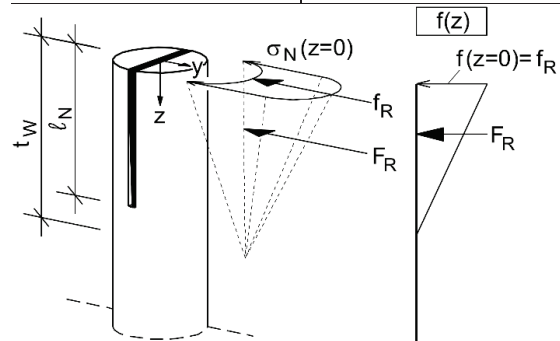
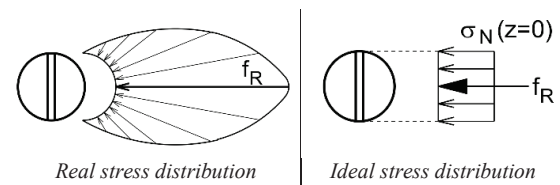


**Figure 6:** Mechanical model of the WWD. Above: Two-dimensional representation of the real (left) and ideal (right) stress distribution on BC's surface  $\sigma_N(z=0) \neq 0$  and linear load distribution  $f_R$ . Below: stress distribution along  $z$ -axis up to  $\sigma_N(z \geq t_w) = 0$  in three-dimensional representation.

Considering the distribution of the stress on BC's surface  $\sigma_N(z=0) \neq 0$  constant along the diameter  $d_D$  of the dowel and the resultant linear load distribution  $f_R$  (2), (3) and taking into account along the z-axis the triangular distribution of the stress up to the maximum depth of load transfer  $t_W$  it is possible to calculate the force  $F_R$  (4) transferred from the wooden wedge's spreading surface to the BC (see Figure 6, below). Considering the force  $F_R$  is applied on the spreading surface with an angle  $\alpha$ , the forces acting perpendicular and parallel to the spreading surface can be calculated from it. Furthermore, the force  $F_R$  activates friction according to Coulomb's law of friction (see Figure 7). The static friction plays a decisive role for the tensile load-bearing capacity of the wooden wedged dowel. In fact, the achievement of the sliding friction is defined as the failure point of the fastener.

$$f(z=0) = f_R \quad \left[ \frac{N}{mm} \right] \quad (2)$$

$$f_R = \sigma_N(z=0) \cdot d_D \quad \left[ \frac{N}{mm} \right] \quad (3)$$

$$F_R = 0.5 \cdot t_W \cdot f_R \quad [N] \quad (4)$$

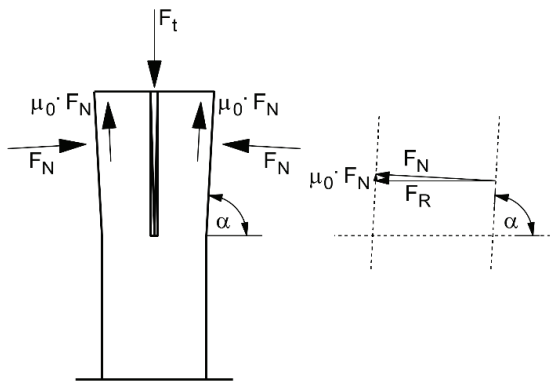


**Figure 7:** Mechanical model of the wooden wedged dowel under tensile stress. Equilibrium of forces due to wedging and tensile stress.

Since the angle  $\alpha$  is very small and it can be considered as approximately a right angle  $\alpha \cong 90^\circ$ , it is defined that  $F_R \cong F_N$  and  $F_N \cdot \mu_0 \cong F_R \cdot \mu_0$ . Therefore, it can be considered that the value of the tensile force  $F_t$  is the one contained in the equation (5)

$$F_t \cong 2 \cdot \mu_0 \cdot F_R \quad [N] \quad (5)$$

It is therefore concluded that, the verification for the repair connection with wood wedged dowels under axial tensile load is the one in following equation (6):

$$F_{t,Rk} = \mu_0 \cdot t_W \cdot k_S \cdot v(z=0) \cdot d_D \quad [N] \quad (6)$$

With:

- $\mu_0$  = friction coefficient between dowel and BC;
- $t_W$  = depth of the wedge action;
- $k_S$  = foundation modulus;
- $v(z=0)$  = maximum displacement of groove on BC's surface;
- $d_D$  = dowel's diameter.

The values to be assigned to the parameters contained in the verification (6) can be found in Table 2.

**Table 2:** Value of the parameters contained in the verification for the repair connection with wooden wedged dowels under axial tensile load.

parameter	condition	parameter description, value	unity
$\mu_0$	H1	$\mu_{0,H1} = 0.5$	[-]
	H2	$\mu_{0,H2} = 0.6$	
	H3	$\mu_{0,H3} = 0.4$	
$t_W$		$t_W = 37.5$	[mm]
$k_S$	H1	$k_{s,H1} = 6.28$	$\left[ \frac{N}{mm^3} \right]$
	H2	$k_{s,H2} = 46.40$	
	H3	$k_{s,H3} = 6.28$	
$v(z=0)$	$d_D = 20$		[mm]
	H1	$v(z=0) = 0.8$	[mm]
	H2	$v(z=0) = 0.2$	
	H3	$v(z=0) = 0.8$	
	$d_D = 30$		[mm]
	H1	$v(z=0) = 0.59$	[mm]
H2	$v(z=0) = 0.12$		
H3	$v(z=0) = 0.64$		
$d_D$		$d_D = 20$	[mm]
		$d_D = 30$	

The model verification for the wooden wedged dowel under axial tensile stress is carried out taking into account the results from the test series V1 [9]. The parameters contained in the Table 2 are the result of observations in the experimental campaigns TV1 [15], and V1, literature and numerical or mathematical calculations in [9]. The parameters are following explained.

The coefficient of static friction wood-wood  $\mu_0$  is found in the literature in the range  $\mu_0 = 0.4 \div 0.6$ . The static friction coefficients for the verification (6) have been defined basing on the test observations for each wood combination. The definition bases on deductions from studies about the dependence of the embedment strength of fasteners from the surface roughness of drift bolts from Sjödin [20].

The depth of the wedge action  $t_W$  was determined from FE-Simulations. The depth of the wedge action defines the depth of load transfer area (A) between the building components and the WWD as in Figure 4. This value is fixed as constant for fasteners with groove's depth  $l_N = 30 \text{ mm}$ , independently from the wood combination. The displacement values on BC's surface  $v(z=0)$  are measured in the experimental campaign V1 [9] for the dowel's diameter  $d_D = 20 \text{ mm}$ , and are result of observations and calculations for dowel's diameter  $d_D = 30 \text{ mm}$ .

The foundation modulus  $k_S$  is the resistance of the wood volume to an applied force. In the literature, only studies on embedment strength by Spörk and Hübner [18, 19, 21]

(for hardwoods) and Blaß [22] (for softwoods) were found. Therefore, the foundation modulus for oak (*Quercus*) and ash (*Fraxinus excelsior*) wedges was experimentally determined according to DIN EN 383:2007 [23]. The dowels are loaded perpendicular to the grains, parallel to the annual rings. The results are in following (7) and (8).

$$k_{S,quercus,90,EN383} = 48,11 \left[ \frac{N}{mm^3} \right] \quad (7)$$

$$k_{S,frax.ex,90,EN383} = 35,31 \left[ \frac{N}{mm^3} \right] \quad (8)$$

The  $k_S$ -value in (7) should be valid for dowels in oak (*Quercus*) for the combination H1, H2, and the  $k_S$ -value in (8) should be valid for dowels in ash (*Fraxinus excelsior*) for the combination H3. Nevertheless, these tests only served to have first values of  $k_S$ . In fact, the  $k_S$ -value from (7) is correct to the large order for the wood combination H2 but not for the H1 so far (see Table 2), although both wood combinations have an oak dowel. Similarly, the  $k_S$ -value from (8) does not agree with the value of  $k_S$  from Table 2 for the wood combination H3. The cause of this incongruities is to be found in the EN 383:2007 [23] itself. Here, the test piece is a rectangular prism of wood loaded by a metallic fastener placed with its axis perpendicular to the surface of the test piece. On the contrary, the foundation modulus in the repair connection with wood wedged dowels is determined, not only by the  $k_S$ -value of one wooden species (the test piece), but especially by the interaction between the foundation moduli of the two encountering wood species, in the dowel and in the building component. These two components are stressing each other at a variable stress angle derived by Spörk in [18, 19] (Figure 8), and the angle and wood species with the lower foundation modulus, or reverse, the higher elasticity, determines the final  $k_S$ -value for the wood combination.

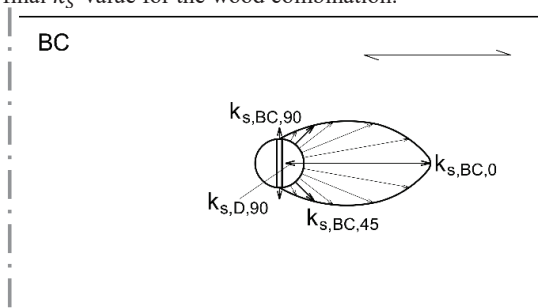


**Figure 8:** Assumptions on elastic behaviour of the dowel and building component in the contact area between the building component and the dowel (wedging interaction area).

Thus, following hypotheses about the stress behavior of the timber combinations are formulated (referring to Figure 8). Assumption for H1 and H3: The elasticity of the BC made of spruce stressed in compression parallel to the grains is greater than the one of the dowel made of oak (in H1) or ash (in H3) stressed in compression perpendicular to the grains (9):

$$k_{S,BC(spruce),0} < k_{S,BC(spruce),45} < k_{S,D(oak/ash),90} \quad (9)$$

Therefore, for the timber combinations H1 and H3, the building component made of spruce determines the properties for the foundation modulus as  $k_{S,BC(spruce),0}$ . Assumption for H2: The elasticity of the oak dowel, stressed in compression perpendicular to the grain, is bigger than that one of the oak building component, stressed in compression parallel to the grain (10):

$$k_{S,D(oak),90} < k_{S,BC(oak),45} < k_{S,BC(oak),0} \quad (10)$$

Therefore, for the timber combination H2, the dowel made of oak, loaded perpendicular to the grains, determines the properties for the foundation modulus as  $k_{S,D(oak),90}$ .

## 4.2 EXPECTED LOAD-BEARING CAPACITY OF WOOD WEDGED DOWELS UNDER AXIAL TENSILE LOAD

In the following Table 3 are reported the load-bearing capacities for one wooden wedged dowel under axial tensile load as fasteners for a carpentry repair connection, in dependence from the wood combination. The expected characteristic values  $R_{k,WWD,mod}$  after the presented model are compared with the 5% quantile of the characteristic values  $R_{k,WWD,exp}$  from the tests V1 [9].

**Table 3:** Characteristic values of load-bearing capacity for wooden wedged dowels under axial tensile load in dependence from the wood combination. Characteristic values of the tests V1 ( $R_{k,WWD,exp}$ ) and the ones after the presented model ( $R_{k,WWD,mod}$ ).

Parameter	condition	parameter description	unity	deviation
$d_D = 20mm$				
$R_{k,WWD,exp}$	H1	1.67	[kN]	
	H2	3.58		
	H3	1.93		
$R_{k,WWD,mod}$	H1	1.88		12.6 %
	H2	4.18		16.8 %
	H3	1.51		-21.8 %
$d_D = 30mm$				
$R_{k,WWD,exp}$	H1	2.49	[kN]	
	H2	3.14		
	H3	2.40		
$R_{k,WWD,mod}$	H1	2.08		-16.5 %
	H2	3.76		19.7 %
	H3	1.81		-24.6 %

In the last column of Table 3 the deviations between the characteristic values of load-carrying capacity from the proposed model and the ones of the experimental results are shown. On one side, the load-carrying capacity for the WWD with smaller diameter  $d_D = 20mm$  is a little overestimated and the one for the bigger diameter  $d_D = 30mm$  is underestimated. The overestimation remains in the tolerance of +20% and the underestimation is on the safe side up to -25%. On the other side, the

experimental results [9] presents a big statistical scatter and the obtained deviation remains in the tolerance of the test results.

Concluding, from the comparison between the results of the proposed model and the experimental results, can be inferred that the proposed model predicts very good the values of load-carrying capacity for the wooden wedged dowel under axial tensile load.

### 4.3 VERIFICATION FOR THE REPAIR CONNECTION WITH WOOD WEDGED DOWELS UNDER SHEAR LOAD

The verification for the repair connection with wooden wedged dowels under single and double shear loading (with one or two shear planes), bases on existing mechanical models and verifications norms [11–13]. More specific, the here proposed verification model bases on the model from Blaß [12] and norm SIA 269/5:2011 [13].

In the experimental campaign SV [9] experimental tests on a mortise and tenon joint with wooden wedged dowels (WWD), and wooden dowels (WD) as mechanical fasteners under double shear have been carried out. The proposed geometric parameters for the tests are wood combination H1 (refer to Table 1) and dowel's cross-section  $d_D = 20\text{mm}$ .

In the Table 4 are reported the characteristic values (5% quantile) of the tests SV carried out in [9] for the WWD and WD. The results show that the load-carrying capacity of the wooden wedged dowels is lower than the one for wooden dowels. Furthermore, in the Table 4 are reported the expected characteristic values of load carrying capacity for the WD and WWD calculated after the model from Blaß in [12]. From the comparison among these values it is clear that, on one side, the model [12] describes very well the test results for the wooden dowels, and on the other side, the results of load carrying capacity for the wooden wedged dowels calculated after [12] are too high in comparison with the test results.

**Table 4:** Characteristic values of strength for repair connection mortise and tenon joint (double shear) with wooden dowels and wooden dowel under shear load: results after model in [12] and experimental test results.

Parameter	condition	parameter value	unity
$R_{k,WWD}$	experimental	6.61	[kN]
	After [12, 13]	8.57	
$R_{k,WD}$	experimental	7.62	[kN]
	After [12, 13]	8.67	

In the verification of wooden dowels from [12, 13] the reduction coefficient  $\delta$ , takes into account the effects of non-linear stress distribution along the borehole, the non-utilization of the embedding strength and rope effects due to friction in the borehole. From the observation of the tests SV [9] was revealed that these side effects are not only evident in wood dowels, but also magnified in wood

wedged dowels under shear stress. The presence of the reduction coefficient  $\delta$  from [12, 13] is therefore particularly interesting for the further development of the verification model for the wood wedged dowels.

In order to update the reduction coefficient  $\delta$ , some explanations about the causes of reduction of the load-carrying capacity in the WWD were given: the reason may lie in the geometry of fasteners' components. The geometry causes firstly a change in the distribution of forces along fasteners' neutral axis and secondly causes a change in the contact area between the building component and the dowel. These phenomena may cause wooden wedged dowels experience earlier shear failure than the wooden dowels. These two hypotheses are following explained.

Hypothesis 1) (refer to Figure 9). During loading the fasteners are generally subjected between the shear joints to bending in the borehole. One half of the fastener's cross section is loaded in compression and the other half in tension; the shear forces are maximum along the neutral axis.

On one side, the WD has a constant cross-section along the entire length and it distributes the shear forces equally along the whole neutral axis' length. On the other side, in the WWD the grooves at two far ends, exactly cut the cross-section in the ending part of the neutral axis into two half cross-sections. Therefore, the WWD presents a shorter neutral axis' length for absorbing the maximum shear force.

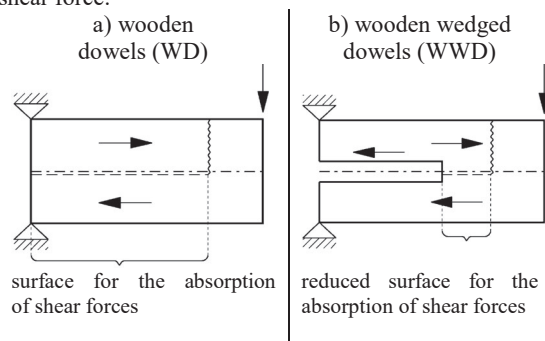


**Figure 9:** Representation of hypothesis 1): assumptions on the absorption of shear forces in the two far ends of the fastener in a) WD and b) WWD.

Hypothesis 2) (refer to Figure 10). During loading the fasteners are generally subjected between the shear joints to bending in the borehole.

On one side, the wooden dowel has no restraints in the borehole except than the skin friction as in the surface (B) described in Figure 4. Therefore, once subjected to bending it can axially shift in the borehole, depending from the contact surface and the presence of imperfections in the geometry. The WD is - mechanically speaking - a displaceable beam in axial direction (see Figure 10a). Referring to the middle wood, the cross-sections of the fasteners are subjected along the neutral axis on the lower half to tensile stress and on the upper half to compression from the bending. On the other side, the wooden wedged dowel (WWD) activates a further load transfer area due to

the wedging; here, the fastener is able to absorb axial tensile forces during loading, as explained in Figure 4. Therefore, once subjected to bending, the WWD cannot axially free shift in the borehole as the WD. The WWD is - mechanically speaking - a non-displaceable beam in axial direction (see Figure 10b). This causes an additional axial tensile stress in the fastener's cross-sections. Referring to the middle wood, the cross sections are here on the lower half not only subjected to tensile stress from bending, but also to additional tensile stress from the wedging and its clamping effect. As a consequence, the neutral axis shifts from fastener's main axis to the upper half of the cross-section. Earlier failure in this zone is expected. In experimental tests SV [9] an additional failure in this area was also observed.

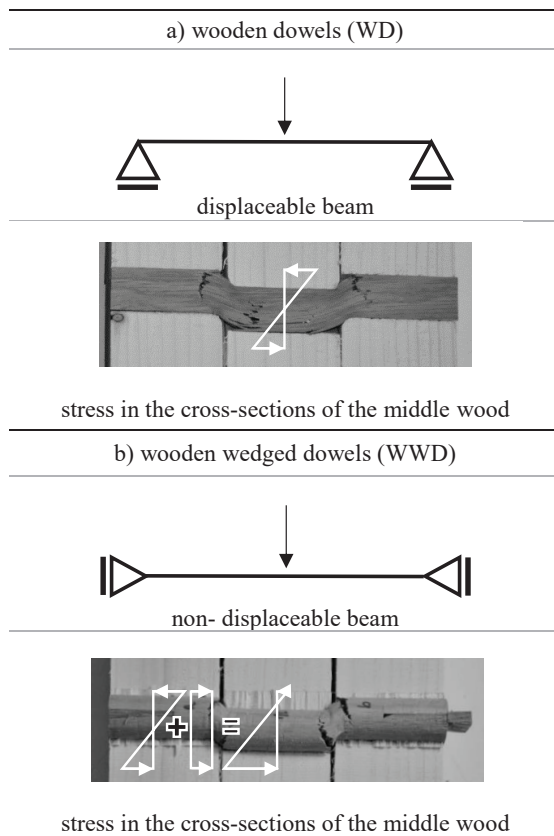


**Figure 10:** Representation of hypothesis 2): mechanical interpretation, and stress in the cross-sections of the middle wood after shear loading in the a) WD and b) WWD.

According to the hypothesis 1 and hypothesis 2, a new reduction coefficient  $\delta'$ , is defined. The reduction coefficient  $\delta'$  considers the effects of non-linear stress distribution along the borehole, the non-utilization of the embedment strength, rope effects due to friction in the borehole, and the additional clamping effect due to the wedging in the WWD. The updating of the reduction coefficient  $\delta'$  is calculated back from the characteristic values (5% quantile) of load-carrying capacity of the experimental tests SV [9] and the known variables from

the equation of Blaß [11]. The new value for the reduction coefficient is determined as:  $\delta' = 0.45$ . The verification model for the wooden wedged dowels under shear load is defined in the following equation (11).

$$R_k = \sqrt{\frac{2 \cdot \beta}{1 + \beta}} \cdot \sqrt{2 \cdot M_{u,k} \cdot \delta' \cdot f_{h,1,k} \cdot d_D} \quad [N] \quad (11)$$

With:

$$\delta' = 0,45 \quad [-] \quad (12)$$

$$\beta = \frac{f_{h,1,k}}{f_{h,2,k}} \quad [-] \quad (13)$$

$$M_{u,k} = \frac{f_{m,k} \cdot \pi \cdot d_D^3}{32} \quad [N \cdot mm] \quad (14)$$

$$f_{h,1,k} = 0,082 \cdot (1 - 0,01 \cdot d_D) \cdot \rho_k \quad \left[ \frac{N}{mm^2} \right] \quad (15)$$

The verification (11) describes the maximum calculated characteristic load-carrying capacity for one fastener and per shear joint. The verification is directly connected with the one from [12, 13]. In (13)  $\beta$  describes the ratio of the embedment strength of the side wood to the middle wood (from SIA 265:2012 [24]); here,  $f_{h,1,k}$  represents the characteristic embedment strength of the side wood and  $f_{h,2,k}$  of the middle wood. In (14)  $M_{u,k}$  describes the characteristic value of bending moment of the cylindrical wooden fasteners; here, the value  $f_{m,k}$  is the value of characteristic bending strength of the wooden fasteners from DIN EN 338 [16]. Finally, the diameter of the wooden wedged dowel is described by  $d_D$  and the bulk density of the side wood by  $\rho_k$ .

As well as for the verification in [12, 13], the value of load-carrying capacity calculated by (11) is valid if the minimum wood thickness of the side wood ( $t_{1,req}$ ) and the one of the middle wood ( $t_{2,req}$ ) are achieved. For a single shear joint the thickness of the side wood 1 and the side wood 2 is determined in the eq. (16) and eq. (17) respectively. For a double shear joint the thickness of the middle wood is further described in the equation (18).

$$t_{1,req} = \left( 2 \cdot \sqrt{\frac{\beta}{1 + \beta}} + 2 \right) \cdot \sqrt{\frac{M_{u,k}}{\delta \cdot f_{h,1,k} \cdot d}} \quad [mm] \quad (16)$$

$$t_{2,req} = \left( 2 \cdot \sqrt{\frac{\beta}{1 + \beta}} + 2 \right) \cdot \sqrt{\frac{M_{u,k}}{\delta \cdot f_{h,2,k} \cdot d}} \quad [mm] \quad (17)$$

$$t_{2,req} = 4 \cdot \sqrt{\frac{\beta}{1 + \beta}} \cdot \sqrt{\frac{M_{u,k}}{\delta \cdot f_{h,2,k} \cdot d}} \quad [mm] \quad (18)$$

If the middle or side woods are thinner than the required minimum timber thicknesses  $t_{i,req}$ , the characteristic load-bearing capacity according to eq. (11) is reduced according to eq. (19)

$$R_{k,red} = R_k \cdot \min \left\{ \begin{array}{l} t_1 \\ t_{1,req} \\ t_2 \\ t_{2,req} \end{array} \right. \quad [mm] \quad (19)$$

#### 4.4 EXPECTED LOAD-BEARING CAPACITY OF WOOD WEDGED DOWELS UNDER DOUBLE SHEAR LOAD

In the Table 5 the estimated maximum load carrying capacity for the wooden dowels  $R_{k,WD,mod}$  is calculated after the model of Blaß [11] and the estimated load-carrying capacity for the wooden wedged dowels  $R_{k,WWD,mod}$  is calculated after the proposed model [9].

**Table 5:** Characteristic values of load-carrying capacity for WWD and WD under double shear load: results after model in [12], after the proposed model and experimental test results. Slip moduli after experimental results.

	Parameter	condition	value	unity
WWD	$R_{k,WWD,exp}$	experimental	6.61	[kN]
	$R_{k,WWD,mod}$	after model [9]	6.61	
	$k_{ser,mean,WWD}$	experimental	12.57	$\left[ \frac{kN}{mm} \right]$
WD	$R_{k,WD,exp}$	experimental	7.62	[kN]
	$R_{k,WD,mod}$	After model [12]	8.67	
	$k_{ser,mean,WD}$	experimental	13.21	$\left[ \frac{kN}{mm} \right]$

The values of the maximum load can be used for the calculation of the slip modulus  $k_{ser,mean}$  for both the repair connection with wooden wedged dowels according to the proposed verification [9], as well as for the repair connection with wooden dowels according to the model in [12]. The slip moduli  $k_{ser,mean}$  presented in the Table 5 are therefore calculated for both the repair connections with WWD and WD according to the norm DIN EN 26891:1991-07 [25].

#### 5 CONCLUSION

Concluding, this paper and the related research project [9] introduce the use of the wooden wedged dowels as mechanical fasteners for carpentry connections and clarify manufacturing rules, geometric boundary conditions, working principles, as well as develop a verification for the prediction of load-carrying capacity for the fasteners under axial tensile and shear load.

Regarding geometric boundary conditions, the definition of manufacturing rules and construction parameters, was fundamental. In fact, different load-carrying capacities are expected in dependence from wood combination and fastener's diameter. Therefore, changing the geometric boundary conditions, divergent results than the presented ones are expected. For this reason, the presented verification models and expected characteristic load-

carrying capacities are valid only under the presented boundary conditions.

Regarding peculiar properties of the fastener wooden wedged dowel, it shows, differently to a normal wooden dowel, an improved contact surface in the borehole given by the clamping effect of the wedge, that always guarantees the load transfer between the fastener and the building component. The clamping effect confers to the fastener a rope effect during the loading. This property of the wooden wedge dowels is advantageous in the case of axial load; however, in case of shear load, the wedging contributes to a reduction of the load-bearing capacity, compared to the load-bearing capacity of an equivalent connection with wooden wedges.

The developed verifications open up for engineers the possibility to apply carpentry repair connections with wooden wedged dowels as fasteners in relevant load cases, for example for hanging ceiling coffer beams (wooden wedged dowels in tensile load), or for ceiling beams and roof rafters (wooden wedged dowels in shear load).

The research project is designed as a long-term project to re-learn and understand historical techniques and carpentry connections in order to promote the "best practice" under static-constructive, economic, culturally oriented aspects in heritage conservation.

#### 6 ACKNOWLEDGEMENT

The research was financed with funds from the research initiative Zukunft Bau of German Federal Institute for Research on Building, Urban Affairs and Spatial Development (BBSR, BMI) (SWD-10.08.18.7-18.16), and of Niedersächsisches Landesamt für Denkmalpflege (NLD).

#### 7 REFERENCES

- [1] G. Schickhofer and U. Hübner, Eds., *Bestandsanalyse und Instandhaltung von Holzkonstruktionen*, 8th ed. Graz, 2009.
- [2] M. Petzet, Ed., *Grundsätze der Denkmalpflege: 1. ICOMOS, Heft des Deutschen Nationalkomitees*. München, 1992.
- [3] ICOMOS and ISCARSAH, Eds., *Grundsätzen zur Erhaltung historischer Holzstrukturen.*, 1999.
- [4] ICOMOS and ISCARSAH, Eds., *Principles for the preservation of historic timber structures*, 1999.
- [5] ICOMOS and ISCARSAH, Eds., *Principles for the conservation of wooden built heritage*, 2017.
- [6] J. Egle, Ed., *Dauerhaftigkeit von Holz bei chemisch- aggressiver Beanspruchung*, 2003.
- [7] Forest Products Laboratory, Ed., *Wood Handbook—Wood as an engineering material. General Technical Report FPL-GTR-190*. Madison, WI.
- [8] Informationsdienst Holz, "Korrosion metallischer Verbindungsmittel in Holz und Holzwerkstoffen," Spezial Februar 2003, 2003.
- [9] E. Perria, S. Siegert, M. Sieder, and Reulecke C., "Holzkeildolle als Reparaturverbindung: Einsatz

- der Holzkeildolle als Möglichkeit neuer Reparaturverbindungen für die Denkmalschutzanforderungen des schonenden Substanzumgangs und der Materialgerechtigkeit,” BBSR, Bonn, (in publication) 2022.
- [10] M. Kessel and R. Augustin, “Untersuchung der Tragfähigkeit von Holzverbindungen mit Holznägeln für Sanierung und Rekonstruktion von alter Bausubstanz, Forschungsbericht,” FH Hildesheim/Holzminde, Fachbereich Bauingenieurwesen, 1992.
- [11] M. Kessel and R. Augustin, “Untersuchung der Tragfähigkeit von Holzverbindungen mit Holznägeln,” *Bauen mit Holz*, no. 96, pp. 484–487, 1994.
- [12] H. J. Blaß, H. Ernst, and H. Werner, “Verbindungen mit Holzstiften - Untersuchungen über die Tragfähigkeit,” *Bauen mit Holz*, vol. 10, pp. 45–52, 1999.
- [13] *Erhaltung von Tragwerken – Holzbau*, SIA 269/5:2011, SIA Schweizerischer Ingenieur und Architektenverein, Zürich, 2011.
- [14] A. Müller, M. Vogel, S. Lang, and F. Sauser, *Historische Holzverbindungen. Untersuchung des Trag- und Verformungsverhaltens von Historischen Holzverbindungen und Erstellung eines Leitfadens für die Baupraxis*: Fachhochschule Biel, 2016.
- [15] Perria E., Siegert S., Li X., Sieder M., “Repair connection with wooden wedged dowels: preliminary experimental laboratory tests and fem model for the description of the mechanical behavior,” in *12th International Conference on Structural Analysis of Historical Constructions SAHC 2020*.
- [16] *Structural timber - Strength classes*, DIN EN 338:2016-07, DIN Deutsches Institut für Normung e.V.
- [17] K. J. Witt, Ed., *Teil 3: Gründungen und geotechnische Bauwerke*, 7th ed.: Ernst & Sohn.
- [18] J. Hohenwarter, *Vergleich der Lochleibungsfestigkeit in Folge von Zug- und Druckbelastung*. Graz, 2014.
- [19] a. Spörk, “Einflussfaktoren auf die Lochleibungsfestigkeit für die Nadelholzart Fichte,” TU Graz, Internes Paper holz.bau forschung gmbh, Mar. 2007.
- [20] J. Sjödin, E. Serrano, and Enquist, Bertil (2008), “An experimental and numerical study of the effect of friction in single dowel joints,” in *Holz als Roh und Werkstoff*, pp. 363–372.
- [21] U. Hübner, Ed., *Mechanische Kenngrößen von Buchen-, Eschen- und Robinienholz für lastabtragende Bauteile*. Graz: Verlag der Technischen Universität Graz, 2013.
- [22] H. J. Blaß, O. Eberhart, and B. Wagner, “Zum rechnerischen Nachweis von Winkelverbindern,” *Bauen mit Holz*, no. 102, pp. 42–46, 2000.
- [23] *Timber Structures — Test methods — Determination of embedment strength and foundation values for dowel type fasteners*, EN 383:2007, DIN Deutsches Institut für Normung e.V., Berlin, 2007.
- [24] *Holzbau*, SIA 265:2012, SIA Schweizerischer Ingenieur- und Architektenverein, Zürich, 2012.
- [25] *Timber structures; joints made with mechanical fasteners; general principles for the determination of strength and deformation characteristics (ISO 6891:1983)*, DIN EN 26891:1991-07, DIN Deutsches Institut für Normung e. V., Jul. 1991.